ANALYSIS OF TRANSIENT TEMPERATURE DISTRIBUTION IN ROTATING ARC GMA WELDING BY CONSIDERING DROPLET DEFLECTION

by Cheolhee Kim[1] and Suck-Joo Na[1]*
[1]Department of Mechanical Engineering, KAIST,
Kusong-dong 373-1, Yusong-gu, Daejon, 305-701, Korea, ckim@kaist.ac.kr

ABSTRACT

This paper presents a mathematical model predicting the temperature distribution in rotating GMA welding. The bead width increases with rotation frequency at the same rotation diameter because the molten droplets are deflected by centrifugal force. The numerical solution is obtained by solving the transient three-dimensional heat conduction equation considering the heat input from the welding arc, cathode heating and molten droplets. Generally in GMA welding the heat input may be assumed as a normally distributed source, but the droplet deflection causes some changes in the heat input distribution.

To estimate the heat flux distribution due to the molten droplet, the contact point where the droplet is transferred on the weld pool surface is calculated from the flight trajectory of the droplets under the arc plasma velocity field obtained from the arc plasma analysis. The numerical analysis shows a tendency of broadened bead width and shallow penetration depth with the increase of rotating frequency. The simulation results are in good agreement with those obtained by the experiments under various welding conditions.

KEYWORDS

GMA welding, rotating arc, temperature distribution, drop deflection

1. Introduction

The high-speed arc rotation mechanism was developed first in Japan and used for narrow gap welding and conventional weld seams such as fillet or V- welds [1-3]. Recently a new rotation mechanism was developed by using a hollow shaft motor designed to be installed in the electrode nozzle and the size and weight of the mechanism can be reduced considerably by using a sufficiently small motor [4-5]. Rotating arc welding has great advantages in terms of improved efficiency of welding processes and a more consistent quality. The advantages include an extensive improvement in precision and response when welding is controlled by an arc sensor for seam tracking and also a large increase in welding speed. Moreover the rotating arc welding can be applied to narrow gap welding and position welding, in which it is difficult to develop an automated process [6].

In this study, the numerical model to predict the temperature distribution in the weldment is investigated using the conduction equation. For rotating arc welding, a flat bead surface and decreased penetration depth is observed because the molten droplets are deflected by centrifugal force. Because the GMA welding process utilizes the consumable electrode, the thermal energy applied to the workpiece consists of two sources : the arc energy distribution generated at the cathode area(workpiece) and the thermal energy of the metal drops detached from the electrode wire[7]. For temperature analysis, the molten drop flight trajectory is calculated using the equation of motion and the contact point where the droplet is transferred on the weld pool surface is determined. Calorimetric experiments have been carried out by many researchers to estimate the efficiency of each energy source and the empirical efficiency from the references is adopted as the heat source for the thermal analysis of weldment [8-9].

2. Drop deflection

The molten drop detached from a consumable wire during GMA welding is accelerated in the arc column mainly by gravity and drag force. In rotating arc welding, the drop has an initial velocity tangent to the circle by the centrifugal force when it detaches and is transferred to the base metal with deflection. The images taken by a high-speed camera show that the diameter of the drops varies between 50% and 150% of the wire size, and the molten droplets are deflected by the centrifugal force, as shown in Fig. 1 [10]. But the rotation of the tip does not have a significant effect on the deflection of wire extension, as shown in Fig. 2.

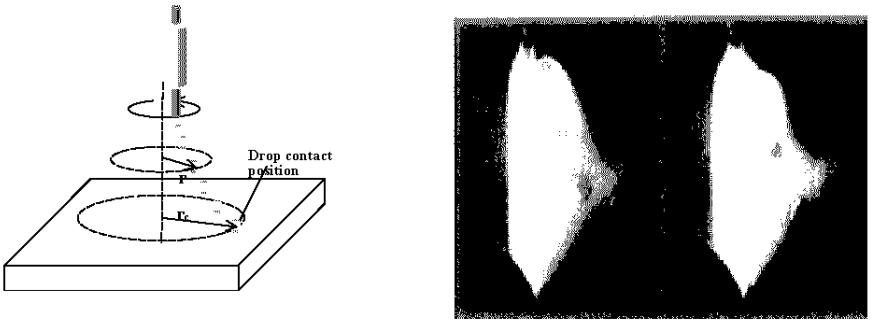

Fig. 1 Drop deflection by the centrifugal force [10]

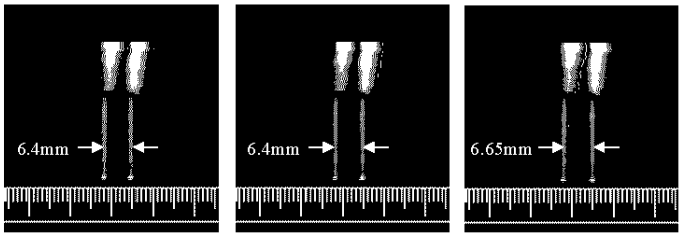

(a) 0Hz (b) 20Hz (c) 40Hz

Fig. 2 Deflection of welding wire in rotating arc welding (D=6mm)

The initial velocity, drag force and gravity are given by the following expressions :

$$v_o = r_a \cdot 2\pi f \qquad (2\text{-}1)$$

$$F_d = C_d A_p \left(\frac{\rho_f v_f^{\,2}}{2} \right) \qquad (2\text{-}2)$$

$$F_g = \frac{4}{3} \pi R_d^{\,3} \rho_d g \qquad (2\text{-}3)$$

where v_o is the initial velocity of the molten drop, F_d the drag force acting on the drop, F_g the gravitational force, r_a the radius of rotation, f the rotation frequency, C_d the drag coefficient, A_P the cross-sectional area of the drop ρ_f the density of the fluid, v_f the velocity of the fluid, R_d the radius of the drop, ρ_d the density of the drop and g the acceleration of gravity.

Because the drag force is dependent on the temperature distribution and velocity distribution of the arc plasma, these distributions are analyzed by the mathematical model developed in an earlier study [11-12]. In the previous study, a two-dimensional and steady-state mathematical model of the gas tungsten arc was investigated by using a code based on a finite difference method. In this study, the arc plasma for GMAW is analyzed by using modified solution domain and boundary conditions as shown in Fig. 3 and Table 1. A more detailed description of the mathematical model and governing equations can be found in the earlier publication [12]. Fig. 4 and Fig. 5 show the velocity and temperature distribution of the arc plasma respectively for GMA welding with a 270A welding current and an 8mm arc length condition. As shown in Fig. 4, the axial velocity is considerably high at the axis of the electrode (z-axis) and decreased rapidly with radial distance.

The flight trajectory of a molten drop is calculated under the assumption that the drop has an equal diameter with the electrode wire. Fig. 6 and Fig. 7 show how the molten drop is deflected at various rotating frequencies and the rotating diameter. Because the molten drop has a greater initial velocity and less drag force with a greater radial distance at the higher frequencies, it is more severely deflected when transferred to the base metal, and the drop contact position on the weld pool surface is located farther away from the center of z-axis.

Table 1 Boundary conditions for analysis of GMA welding arc

	u	w	h	ϕ
AB	0	$\partial w / \partial r = 0$	$\partial h / \partial r = 0$	$\partial \phi / \partial r = 0$
BC	0	0	$h = h_{const}$ $(T = 1000K)$	$\phi = \phi_{const}$
CD or DE	$\partial(\rho r u) / \partial r = 0$	$\partial w / \partial r = 0$	$\partial h / \partial r = 0$	$\partial \phi / \partial r = 0$
EF or DG	0	$w = w_{given}$	$h = h_{const}$ $(T = 1000K)$	$\partial \phi / \partial z = 0$
GA or FA	0	0	$h = h_{const}$ $(T = 1810K)$	$j_n = j(s)_{given}$

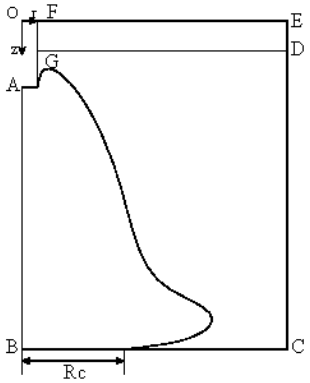

Fig. 3 Solution domain for analyzing GMA welding arc

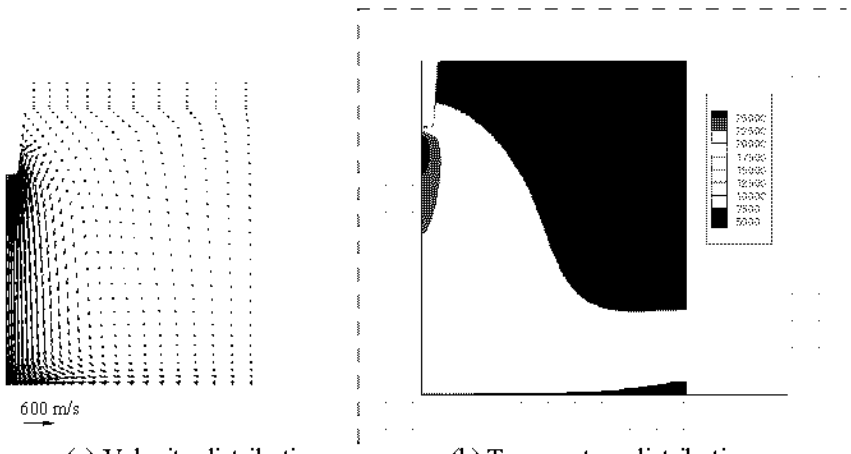

(a) Velocity distribution (b) Temperature distribution

Fig. 4 Results of analysis (270A, 8mm arc)

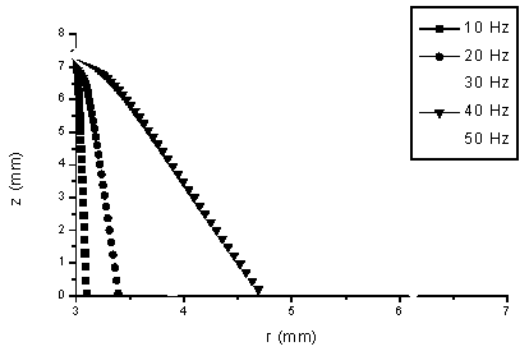

Fig. 5 Drop flight trajectory (270A, D = 6mm)

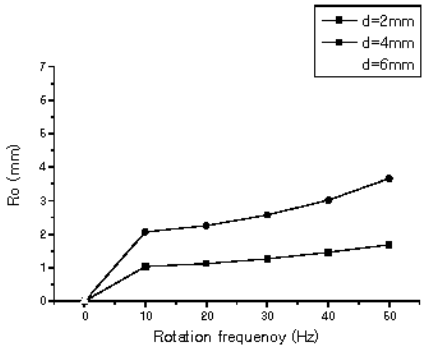

Fig. 6 Drop contact position

3. Temperature distribution

The transient temperature distribution in the base plate is analyzed by applying the heat conduction theory. The computation is performed with the finite element program SYSWELD, which was developed for the thermal analysis of welds[13]. Fig. 7 shows the finite-element mesh adopted for thermal analysis of the base plate and the coordinate system.

The energy equation of the problem is:

$$\rho(T)C_p(T)\frac{\partial T}{\partial t} = \nabla\cdot(k(T)\nabla T) \qquad (3\text{-}1)$$

Boundary conditions of heat flux at the upper surface and other surfaces are given respectively by the following expressions.

$$k_n\frac{\partial T}{\partial n} = -(q_a + q_d) + h_1(T - T_0) + \sigma\varepsilon(T^4 - T_0^4) \qquad (3\text{-}2)$$

$$k_n\frac{\partial T}{\partial n} = h_2(T - T_0) + \sigma\varepsilon(T^4 - T_0^4) \qquad (3\text{-}3)$$

As shown in Fig.8, the forced convection by the shielding gas flow and heat transfer from the heat sources - arc and molten drop are considered at the upper surface and the natural convection is considered at other surfaces.

Each heat source is assumed as the Gaussian distribution and the heat flux from the welding arc, q_a and the heat flux from the molten drop, q_d can be expressed as the following equations.

$$q_a(r) = \frac{3Q_a}{\pi\bar{r}_a}\exp\left[-3\left(\frac{r}{\bar{r}_a}\right)^2\right] \qquad (3\text{-}4)$$

$$q_d(r) = \frac{3Q_d}{\pi\bar{r}_d}\exp\left[-3\left(\frac{r}{\bar{r}_d}\right)^2\right] \qquad (3\text{-}5)$$

where Q is the total heat input into the base metal per unit of time, $\bar{r}$ an effective radius of heat density distribution and r the distance from the center of the heat source. The center of heat input from the welding arc is determined by rotation of the electrode wire and the center of heat input from the molten droplet is located at the drop contact position calculated in the previous section.

The total heat input, Q is determined from the total energy input for GMA welding (IV) and the efficiency of each heat input(η). In this study, 54% for η_a and 17% for η_d are adopted from the experimental results of the previous study by Essers, *et al*[8].

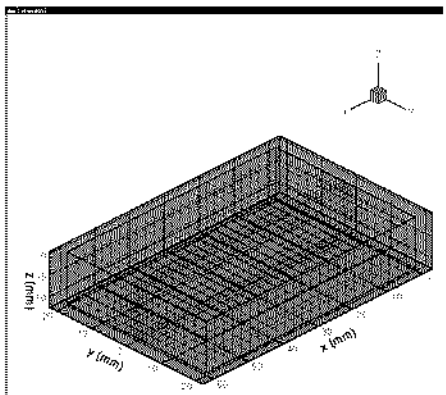

Fig. 7 Mesh generation for thermal analysis

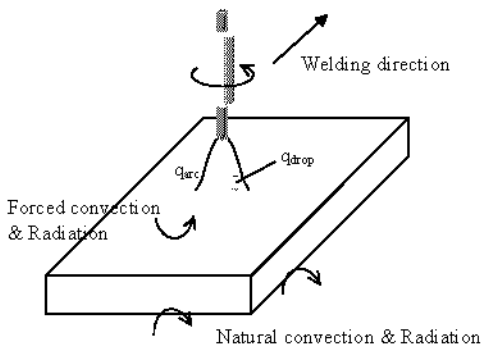

Fig. 8 Boundary conditions for thermal analysis

In the transient analysis of bead-on-plate welding, the bead width and penetration are maintained after 5 seconds from the start of welding. To investigate the influence of the rotation frequency on the weld bead shape, the thermal analyses are carried out for 5 seconds at various rotating frequencies. The melting lines are obtained by projecting the fusion boundary to the y-z plane and compared with the cross-sectional bead shape, as shown in Fig. 9. Fig. 10 shows the calculated and analyzed bead width and penetration depth. The results show that the bead width increases, and the penetration depth decreases, with the rotating frequency by the deflection of the drop.

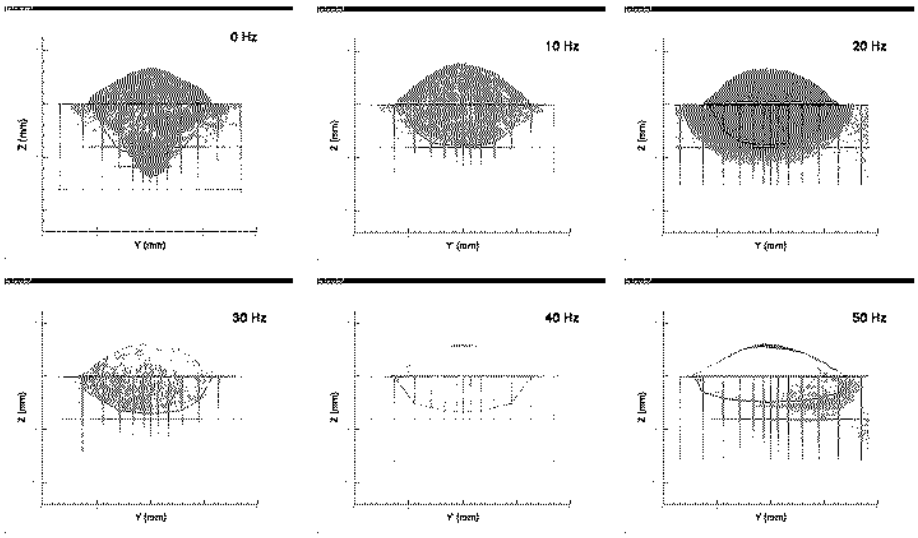

Fig. 9 Influence of the rotation frequency on melting lines of workpiece

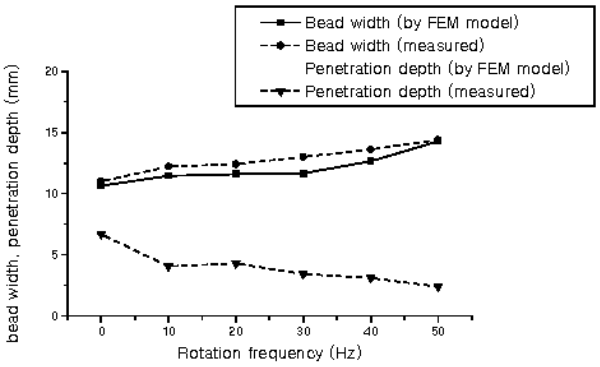

Fig. 10 Calculated bead width and penetration depth

4. Conclusion

In this study, the weld bead characteristics for rating arc welding were analyzed by the numerical method. Because the molten drop deflects when it is transferred to the base metal, the drop deflection under the arc plasma was calculated by using the equation of motion and the drop contact point was used for the center of heat input from the droplet in the analysis. The numerical model with two separate heat sources – from the welding arc and the molten droplet – predicted increased bead width and decreased penetration depth and showed good agreement with experimental results.

Acknowledgements

The authors would like to thank the Ministry of Science and Technology, Korea, for the financial support by a grant from the Critical Technology 21 Project.

References

[1] H. Nomura, Y. Sugitani and Y. Kobayashi: IIW document 12-527-82(1982).
[2] Y. Sugitani, Y. Kobayashi and M. Murayama: Welding International, 7(1991), p.577.
[3] U. Dilthey, M. Oster and J. Gollinick: Welding and Cutting, 48 (1996), P.866.
[4] S.-J. Na, H.-S. Moon and C.-H. Kim: Korean Patent 236916, October(1999)
[5] C.-H. Kim and S.-J. Na: PIME, part B, 215(2001), p.1280.
[6] S.-J. Na, C.-H. Kim and Y.-H. Kang: IURS 2002, June(2002), p.111.
[7] ASM Handbook, 6, 1993
[8] W. G. Essers and R. Walter: Welding Journal, 60(1981), p.37s.
[9] M. J. Lu and S. Kou: Welding Journal, 68(1989), p. 452s.
[10] M. Oster: Ph.D. Dissertaion, Aachen, April(1995)
[11] J. F. Lancaster: Physics of welding, 2nd Ed., 1986
[12] S. Y. Lee and S.-J. Na: Welding Journal, 75(1996), p. 269s
[13] ESI Group, SYSWELD Reference Manual, 1999